Fatigue strength of Al alloy cold sprayed with nanocrystalline powders

Ramin Ghelichi [a,*], Sara Bagherifard [a], Daniel Mac Donald [b], Mathieu Brochu [c], Hamid Jahed [d], Bertrand Jodoin [b], Mario Guagliano [a]

[a] Politecnico di Milano, Via G. la Masa, 1, Milan 20156, Italy
[b] University of Ottawa, 770 King Edward, Ottawa, ON K1N 6N5, Canada
[c] McGill University, 845 Sherbrooke Street West, Montreal, Quebec H3A 2T5, Canada
[d] University of Waterloo, 200 University Avenue West, Waterloo, Ontario N2L3G1, Canada

Article history:
Received 26 January 2013
Received in revised form 4 September 2013
Accepted 5 September 2013
Available online 12 September 2013

1. Introduction

Nanocrystalline (NC) metals are known for their significantly high strength. Surface coating of structural metals with NC materials is expected to improve their mechanical performance. Developing and understanding the damage tolerance of NC coatings are therefore essential for evaluating their overall functionality as structural materials in engineering components.

There are very few studies in the literature on fatigue strength of NC coatings. Hanlon et al. [1] studied the fatigue response of electro-deposited NC pure Ni and cryomilled ultrafine crystalline Al–Mg alloy. The fatigue crack growth experiments on NC and ultrafine crystalline (UFC) coatings were conducted using edge notched samples. It was reported that grain refinement generally led to an increase in resistance to failure under stress controlled fatigue, whereas a deleterious effect was observed on the resistance to fatigue crack growth. Ibrahim et al. [2] studied the fatigue behavior of nanostructured and conventional titania (TiO2) coatings thermally sprayed using air plasma spray (APS) and high velocity oxy-fuel (HVOF) processes onto low-carbon steel (AISI 1018) substrates. They showed that the nanostructured titania coated samples exhibited significantly higher fatigue strength compared to the conventionally sprayed titania partly due to the NC characteristics and partly due to the HVOF process [2].

Cold spray is an innovative coating technique in which metallic particles (10–50 μm) are deposited on metallic substrates [3]. The particle velocity, which results in high kinetic energy, plays an important role in bonding occurrence. The bonding happens in solid state when the particle velocity exceeds a critical velocity [4] and there is no melting; thus, compared to thermal spray coating methods no or negligible oxidation is reported in the coated material. Fig. 1 shows a schematic view of cold spray system and the coating process. In this figure, *P, d*, and *l* are pressure, diameter and length of the nozzle respectively; subscript *e, t,* and *i* are related to exit, throat, and input of the nozzle. The high velocity gas flow is obtained by passing a gas through a convergent–divergent (de Laval) nozzle. Cold spray coatings are becoming highly demanded in many different fields such as biomechanical and aeronautic industries. It is being used for many different surface improvement purposes such as corrosion resistance, wear resistance, or even dimensional restoration and repairing techniques. Direct use of nano size powders as feedstock powder in cold spray, due to the presence of the back flow, is not possible [3]. However, NC powders in micron size agglomerates are reported to be successfully used in cold spray coating by Ajdelsztajn et al. [5]. The hardness of coated NC–Ni is comparable with other NC coating

* Corresponding author.
E-mail addresses: ramin.ghelichi@polimi.it (R. Ghelichi), sara.bagherifard@polimi.it (S. Bagherifard), daniel.macdonald@uottawa.ca (D. Mac Donald), mathieu.brochu@mcgill.ca (M. Brochu), hjahed@uwaterloo.ca (H. Jahed), bertrand.jodoin@uottawa.ca (B. Jodoin), mario.guagliano@polimi.it (M. Guagliano).

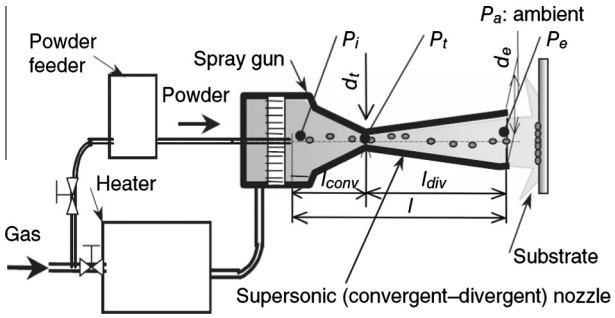

Fig. 1. Schematic view of the machine and bounding of material in cold spray coating [3].

producing techniques such as electro-deposition. Cold spraying has also been successfully used to obtain highly dense NC copper alumina metal matrix composite coatings [6].

Considering the advantages of cold spray to other spray coating processes and the superior physical and mechanical characteristics of NC materials, it is expected that NC coatings can offer the potential for significant improvements in most engineering properties; especially fatigue strength. Furthermore, cold spray coating as an impact based process, induces compressive residual stresses in the substrate [7,8] which shall in turn result in additional fatigue strength improvement. However, to the best of the authors' knowledge, there are no reports yet of cold spray NC metals being used for fatigue experiments, as reported also by Padilla and Boyce [9].

There is even very limited published literature on fatigue strength of conventionally cold spray coated samples (with micron size powder). Price et al. [10] have reported a decrease in fatigue resistance of Ti6Al4 V alloy substrates cold sprayed with pure titanium. This fatigue strength decrease was reported to be due to the substrate-coating interface properties [10]. The effect of cold spray Al–13Co–26Ce coating on the fatigue strength of Al2024-T3 has been studied by Sansoucy et al. [11], who reported notable improvement in fatigue endurance of the coated samples. Ghelichi et al. [8] studied the fatigue behavior of Al5052 samples coated with pure Al and Al7075 feedstock powder. The results indicated good bonding between the coating and the substrate as well as significant fatigue strength improvement up to 30% in the case of Al7075 coatings. The fatigue test data showed a strong dependency of the fatigue strength on the deposited material and the spray parameters [8]. Al-Mangour et al. [12] studied the fatigue strength of annealed low-carbon stainless steel 316L cold sprayed coating. Their results showed the fatigue life of cold spray coatings was lower than bulk material. Compressive stresses found within the coating were reported to be too low to prevent fatigue crack formation and eventually the poor fatigue resistance was related to incomplete particle–particle bonding [12]. Mahmoudi et al. [13] have also reported fatigue life improvement of annealed magnesium AZ31B cold spray coated with aluminum powder.

This paper presents the results of a study on the effect of feedstock powders' structure on fatigue strength of cold spray coated samples. In this regard, Al5042 samples have been coated with Al7075 micron size powders with both micro and nanocrystalline structure. There is a general agreement that grit blasting can increase the deposition efficiency of the coating material by increasing the substrate roughness and thus enhancing mechanical anchoring [8,10,14,15]; thus grit blasting is frequently used as a preliminary treatment before cold spray coating, considering that it also induces compressive residual stresses in the substrate. In this study, all the substrates were grit blasted before coating process. The coated samples have been tested through pure bending fatigue test. Characterization tests such as X-ray diffraction (XRD) measurement for residual stress and grain size, surface roughness, microhardness measurements, and scanning electron microscopy (SEM) observation of fracture surfaces have been performed on the coated samples and reported herein.

2. Materials and experiments

2.1. Material and specifications

The materials considered in this study are Al5052, Al7075, and Al7075CM cryomilled powders. Al-5052, a high strength non-heat-treatable alloy with fatigue strength of about 110 MPa has been chosen as the substrate to be coated. This alloy is a good choice for structures subjected to dynamic vibration. Aluminum alloy 7075, chosen as the powders, is an alloy with zinc as the primary alloying element. It is strong, with strength comparable to many steels, and has good fatigue strength and average machinability, but has less resistance to corrosion than many other Al alloys. Material specifications and chemical composition are given in Tables 1 and 2 respectively.

2.2. Coating procedure

Coating was performed at the University of Ottawa (ON, Canada), using a commercially available low pressure cold spray system [17] produced by SST Centerline Ltd, Winsdor (Canada). All samples have been grit blasted before coating to provide an increased surface area for mechanical bonding of the coating to the substrate. The samples are grit blasted by 18 oz. hopper gravity feed abrasive blaster gun until the surface appeared uniformly worked. The Al-7075 powders were cryomilled (180 RPM rotating velocity) with 820 g of spherical powders with ball to powder weight ratio (mass of milling media: mass of powder) of 32:1; 2.6 g steric Acid (0.35 wt% powder) has been used in order to prevent the welding of the powder to the canister and impeller. Table 3 shows the coating parameters for each set of samples.

Table 1
Nominal properties of the two aluminum alloys [16].

	Hardness (Brinell)	Elastic modulus (GPa)	Elongation at rupture (%)	Poisson ratio	Yield strength (MPa)	Ultimate strength (MPa)
Al5052–O	47	70.3	30	0.33	89.6	193
Al7075–T73	135	72	13	0.33	435	505

Table 2
Chemical composition of the two aluminum alloys (wt%).

	Cr	Cu	Fe	Mg	Mn	Si	Ti	Zn
Al5052–O	0.18–0.28	1.2–2	<0.5	2.1–2.9	<0.3	<0.4	<0.2	5.1–6.1
Al7075–T73	0.15–0.35	<0.1	<0.4	2.2–2.8	<0.1	<0.25	–	<0.1

Table 3
Spray parameters used for the two feedstock powders.

Substrate	Spray parameters	Al7075[b]	Al7075CM[c]
Al5052[a]	Pressure (bar)	16	17
	Temperature (°C)	500	500
	Standoff distance(mm)	15	15
	Feeder rotation (rpm)	3	3
	Gas	N_2	N_2
	Traverse velocity (mm/s)	20	20
	Nozzle length (mm)	120	120
	Nozzle throat diameter (mm)	2	2
	Nozzle exit diameter (mm)	6.3	6.3

[a] Al5052: Mg 2.2–2.8%, Cr 0.15–0.35%, Cu, Fe, Mn max 0.1–0.4. Yield strength: 255 MPa.
[b] Al7075: Mg 2.1–2.9%, Cr 0.18–0.28%, Cu 1.2–2%, Fe 0.5%. Yield strength: 503 MPa.
[c] Cryomilled powders.

2.3. Samples and testing apparatus

The samples for fatigue test were designed based on ASTM B593-96 [18]. Fig. 2 shows the detailed design of a coated sample used for fatigue tests. A costume-built electro-mechanical machine was used for load control pure bending fatigue tests at Mechanical Eng. Lab of Politecnico di Milano University [19]. The system includes an electro-mechanical shaker, a load cell, a controller, dedicated software, and an external metallic structure to clamp the sample. The machine is able to apply cyclic load to the sample at a constant frequency in accordance with the standard requirements. The hardware aspect includes the test machine composed of a LDS (a category of air-cooled electro dynamic shakers which are suitable for vibration testing of small to medium sized payloads) type V406A electrodynamics shaker and a reaction structure to which the specimen is rigidly connected. The main characteristics of the shaker are summarized in Table 4.

A finite element (FE) study was performed on the sample geometry proposed by ASTM B593-96 [18] to examine the homogeneity of stress distribution along its reduced section. The FE results as shown in Fig. 3 indicate the existence of a slight stress concentration on the edge of the sample based on its Von-Mises stress distribution. The numerical solution has been verified using strain gauges on both the edge and the symmetry line of the sample during the test as shown in Fig. 4. The stress concentration factor of the sample was measured to be "1.13" numerically and "1.10" experimentally. The slight difference might be due to the small distance between the position of the strain gauge and the sample edge, which could not be practically avoided; thus, the value obtained through numerical approaches has been used for modifying the final results of the fatigue test.

Table 4
The LSD V406A shaker main features [19].

Specification	Limits
Min frequency	2 Hz
Natural frequency	9000 Hz
Max displacement	17.6 mm
Max velocity	1.78 m/s
Max acceleration	490 m/s^2
Max force	100 N

2.4. Test procedures

Bending fatigue tests ($R = -1$) have been performed at room temperature at a nominal frequency of 90 Hz on grit blasted Al5052 samples: coated with Al7075 microcrystalline powder and coated with Al7075 cryomilled powder. The results of uncoated grit blasted samples are reported for comparison. Each series consisted of 15 samples. The run out limit for the fatigue test was considered 10^7 cycles. The "brief staircase" method presented by Dixon and Massey [20] was used for performing the tests with a stress step of 10 MPa for coated samples, while the results of the uncoated grit blasted samples are obtained from tests performed with a stress step of 20 MPa; these data are reported for comparison [8]. Hodge–Rosenblatt [21] method was used to calculate the fatigue strength corresponding to a fatigue life of 10^7 cycles. The fatigue test data has been elaborated based on the ASTM standard E739-10 [22] to obtain the *S–N* diagram for different cases with a failure probability of 50% on a bi-logarithmic scale.

Microhardness tests have been performed by static indentations made with Vickers diamond pyramid indenter applying load of 50 gf with 15 s dwell time.

Residual stress measurements and also grain size estimation have been performed by XRD diffraction test using X-Stress 3000 X-ray diffraction (radiation Cr Kα, irradiated area 3.14 mm^2, $\sin^2\psi$ method, diffraction angles (2θ) scanned between $\Psi = -45$ and $\Psi = 45$). Measurements have been carried out in depth step by step by removing a very thin layer of material (0.01/0.02 mm) using an electro-polishing device in order to obtain the in-depth profile of residual stresses. A solution of acid acetic (94%) and acid perchloric (6%) has been used for electro-polishing.

The results obtained from diffraction have been used also for grain size measurement based on the single peak analysis method presented by Keijser [23]. This method assumes the XRD pattern as a Voigt function [23,24] that is convolution of a gaussian component regarding microstrain as a Lorenzian (Cauchy) function for grain size.

The microstructure of the samples has been characterized through SEM observation of the feedstock powder and fracture surfaces.

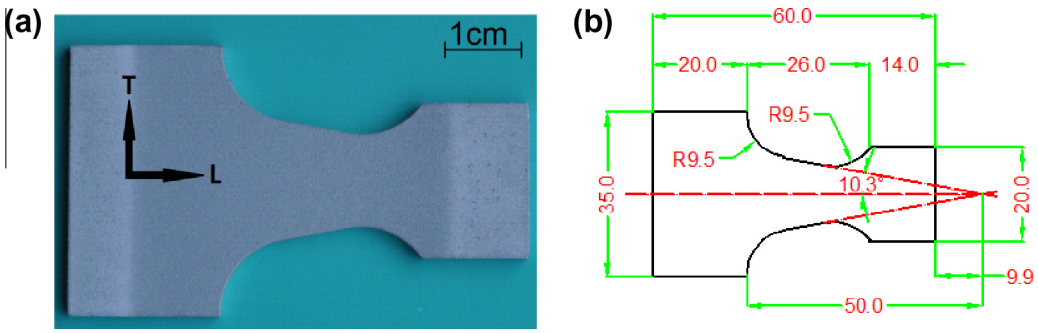

Fig. 2. Fatigue test sample (a) view of a prepared sample and (b) detail design [17].

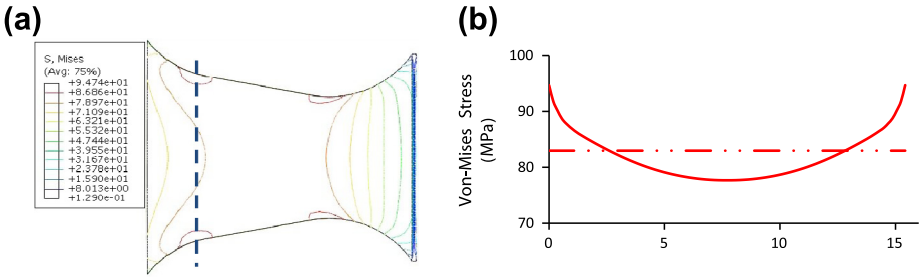

Fig. 3. Stress distribution in the sample (a) Von-Mises contour and (b) Von-Mises stress along the dashed blue line in 3a (in 3b solid line represents the FEM results and dashed line is for the theoretical value). (For interpretation of the references to color in this figure legend, the reader is referred to the web version of this article.)

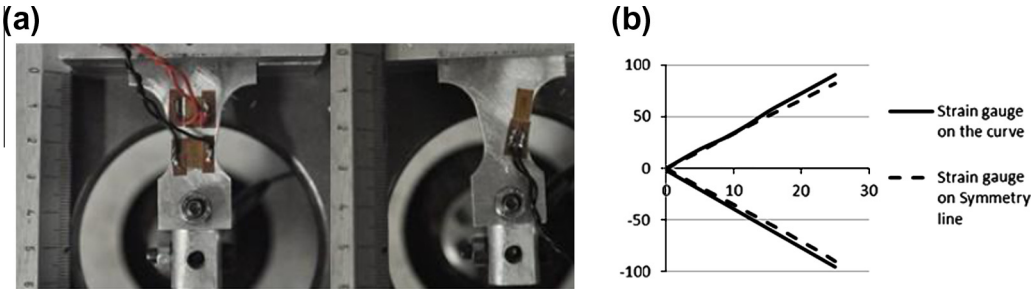

Fig. 4. (a) strain gauge on the specimen and (b) comparison of different strain gauges' results.

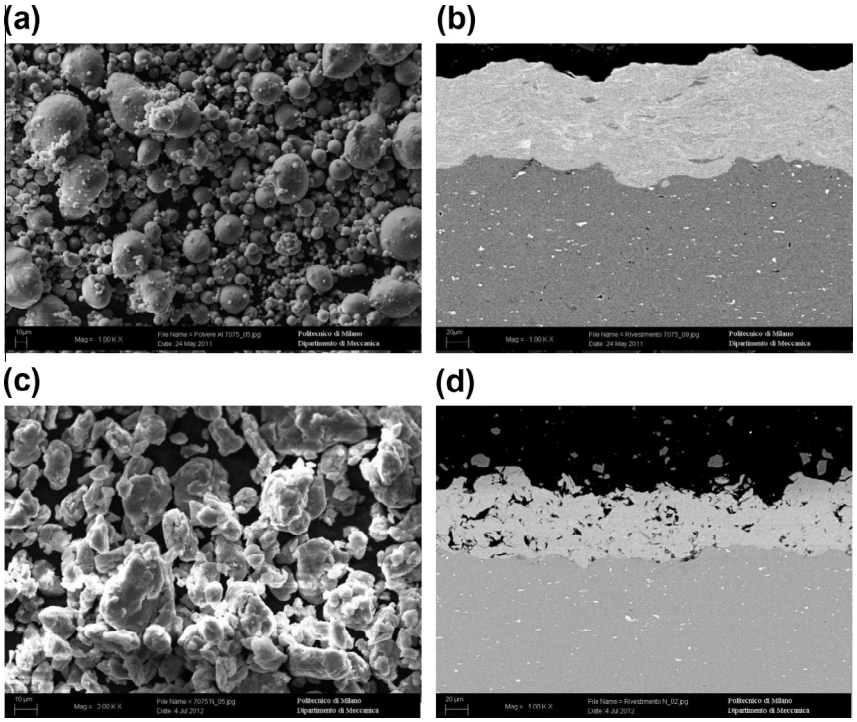

Fig. 5. SEM observation of the feedstock particles and section of coated samples (a) Al7075 microcrystalline particles (b) samples coated with microcrystalline Al7075 (c) Al7075 cryomilled powders and (d) samples coated with cryomilled powders.

3. Results and discussion

3.1. Microstructure analysis

Fig. 5 shows the SEM images of the powders and the microstructure of the sections of the corresponding coated material. There were two powders: micro and nanocrystalline powders (Fig. 5a and c) that were coated on Al5052 substrates (Fig. 5b and d).

As it is shown in Fig. 5a the deposited layer of material for microcrystalline Al7075 is fairly dense with almost no porosity (Fig. 5b). On the other hand, the porosity in the cryomilled coating is measured to be more than 10% (Fig. 5d). The powder image shows the microcrystalline Al7075 particles are almost spherical

while the cryomilled particles have a clearly distorted shape, due to the milling process they have gone through for nanocrystallization. The nanostructure of the powders is not visible in the SEM image due to limitation of the SEM resolution and magnification.

3.2. Residual stress and microhardness

The result of residual stress distribution through the thickness of the grit blasted uncoated sample as well as grit blasted samples coated by microcrystalline and cryomilled Al7075 powders are presented in Fig. 6a. The measurements have been performed on one sample for each series in three different directions (longitudinal (0°), transversal (90°) and 45°) and the average, min and max values of all measurements at each depth are reported in Fig. 6. In this figure the *Y*-axis origin shows approximate location of the interface, with negative length representing the coating. The black lines show the results for the samples coated with microcrystalline powder; red lines show the results for the samples coated with cryomilled powder and the blue line is for the grit blasted samples. The dashed lines for all cases show the range (the min and max values among the measurements on the three directions at each depth) of the stress XRD measurements while the solid lines are representing the average of all measurements at each depth. In depth measurements show the presence of notable compressive residual stresses in the substrate that can be largely due to the grit blasting treatment and also the peening effect of cold spray process. It is also postulated that the treatment parameters particularly the gas temperature can play an annealing role and result in partial relaxation of residual stresses induced by grit blasting and impact of the particles. Indeed the notable difference between the compressive residual stresses after grit blasting and after cold spray coating confirms this hypothesis. Different trends can be observed for the deposited material, interface, and substrate. In residual stress profile, two different peaks are observed for deposited material and the substrate. It can be deduced that there is a slight relaxation in residual stress profile in the interface of the substrate and the coating. Regardless how the residual stresses have been generated in the coating and the substrate, it is well-known that presence of compressive residual stresses can have favorable effects in retarding crack propagation under fatigue loading.

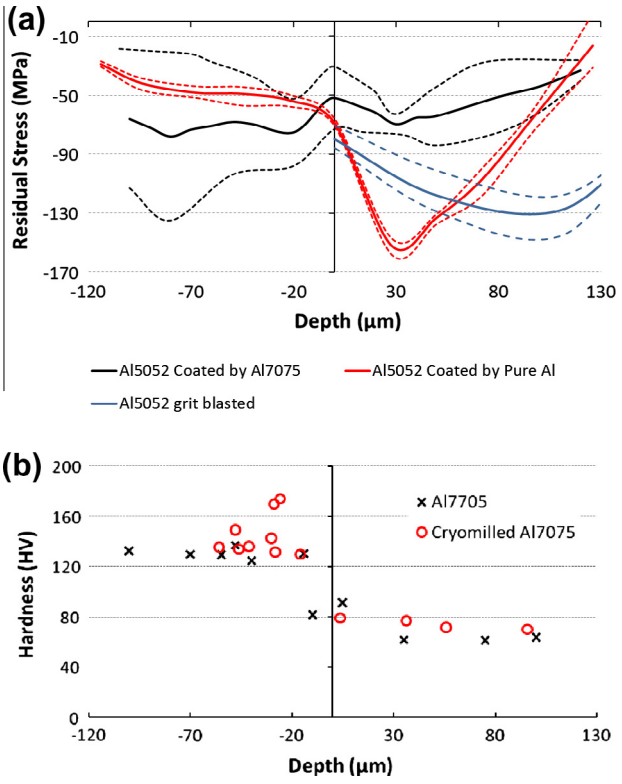

Fig. 6. In depth measurements performed on the samples (a) residual stress (b) hardness (The dashed lines indicate the margin of min and maximum values measured at each depth; the Y-axis origin shows approximate position of the interface, with negative length representing the coating).

The trend of microhardness through the thickness of the sample is also presented in Fig. 6b. It is shown that the hardness in the coating is almost twice that of the substrate. Also in this case the higher hardness in the coating is expected to result in fatigue strength.

3.3. Surface roughness

The other effective parameter on the fatigue endurance of the structure is the surface roughness. Table 5 presents the measured surface roughness for different sets of the samples. The presented data are average of three measurements performed on randomly chosen different positions of samples surfaces. The measurements have been performed both in lateral (L) and transversal (T) directions.

The higher surface roughness measured on the series coated by nanocrystalline powder can be partly attributed to the morphology of the cryomilled powders and the highly distorted shape of the particles after cryomilling process.

3.4. Grain size

Grain size measurement is performed in order to confirm the presence of the NC grains on the samples coated with cryomilled powders. The results of the XRD measurements have been used for grain size measurement by applying the Keijser method [23]. This method is based on representing the experimental XRD spectra by a Voigt profile resulting from the convolution of two broadening mechanisms which would produce a Gaussian profile and a Cauchy (Lorentzian) profile [23,24]. The correctness of the method has been verified by considering four practical cases of size-strain broadening: (i) cold worked nickel, (ii) a nitrided steel (iii) an electro-deposited nickel layer and (iv) a liquid-quenched AlSi alloy and consistent results have been reported [23].

The obtained crystallite size (D) as well as half the maximum height of the peak in the XRD spectra (FWHM) that is directly affected by grain size are presented in Table 6 for cryomilled samples.

The measurements show that the original grit blasted samples have crystal size in the micrometer range and confirm that the crystallite size of the cryomilled powders are in the nano range. The results also show the corresponding FWHM values indicating increase in the peak broadening by decreasing the grain size. It is also interesting to note that the crystal size and the FWHM parameters are not altered after deposition indicating that the plastic deformation occurring during the deposition process does not result in extra crystal refinement.

3.5. Fatigue tests

The brief staircase method [20, 21, 22] has been chosen for calculating the fatigue limit by testing 15 samples for each series; the step for the stress was set to 10 MPa. The tests were also performed for the low cycle part of the *S–N* diagram, by testing more samples with higher loads. Fig. 7 shows the *S–N* diagram obtained for different sets of the samples. The results of grit blasted Al5052 from a previous study of the authors that has been performed with exactly

Table 5
Surface roughness of samples.

Sample	Average thickness[a] (mm)	Measuring direction[b]	R_a[c] (μm)	R_q[d] (μm)	R_z[e] (μm)	R_t[f] (μm)
Grit blasted	2.26	L	4.89	6.20	28.74	39.38
		T	4.95	6.18	27.91	34.58
Grit blasted and coated with microcrystalline Al7075	2.41	L	5.71	7.41	33.61	45.23
		T	5.56	7.25	31.57	47.93
Grit blasted and coated with nanocrystalline Al7075	2.41	L	6.88	8.67	40.60	52.77
		T	7.16	8.94	40.91	51.68

[a] The average of the measured minimum thickness for all samples of each series.
[b] Measuring direction is based on the Fig. 2a.
[c] Arithmetic average [25].
[d] Root mean square [25].
[e] Average distance from highest peak and lowest valley in each sampling length [25].
[f] Maximum height of the profile [25].

Table 6
The crystallite size for the substrate, the coating and the cryomilled powders.

	Grit blasted sample	Cryomilled powders	Deposited material
FWHM (°)	1.23	1.78	1.78
D (nm)	>1000	<50	<50

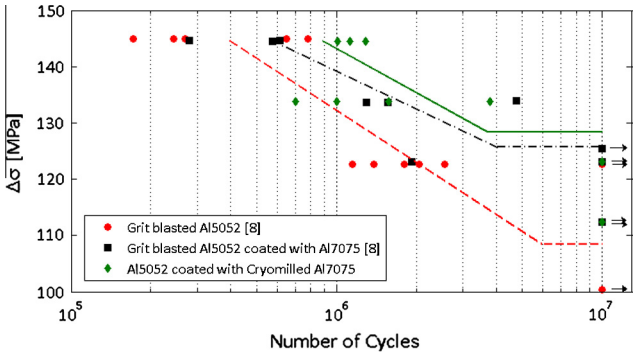

Fig. 7. *S–N* diagram obtained from fatigue test.

the same testing condition apart from the stress step [8] is also added for comparison.

The results presented in Fig. 7 show an improvement for coated samples with respect to grit blasted samples. The fatigue strength of the coated series show improvement of 13% and 20% with respect to the grit blasted ones. In the end, the samples coated by NC cryomilled powder represent a very slight fatigue life improvement with respect to the ones coated with microcrystalline powders, although the difference in the fatigue limits between the two coated series can be considered trivial.

3.6. SEM fractography observations

Fig. 8 shows the fractography images of coated samples. Both fracture surfaces represent ductile fracture marks. The highly deformed coating particles are clearly observed in Fig. 8. Fig. 8a, shows the SEM image of an Al5052 sample coated with Al7075 microcrystalline powders. It can be seen that there is no delamination between the coating and the substrate and there are still bonds between the two. Fig. 8b, on the other hand shows that the deposited cryomilled material has been delaminated from the substrate which may be due to the coating parameters that were insufficient to deform properly the cryomilled powder thus minimizing the particle substrate bonding; i.e. the milled powder are already deformed in the milling process so they have undergone cold working and thus it is expected that they would require a higher velocity at the impact to result in similar deformation and bonding than micro-crystalline powder but since the same spray parameters are used the bonding is not strong enough. As it was observed in the SEM images of coated samples' cross section (Fig. 5), the cryomilled coating is fairly porous; thus it can easily break due to high stress concentration at pores, leading to premature delamination.

4. Conclusions

Effects of cold spray coating and microstructural characteristics of the feedstock powder on fatigue behavior of cold spray coated Al5052 samples have been studied experimentally. Al5052 grit blasted substrates have been coated with Al7075 powder with two different grain size and structures: microcrystalline and nanocrystalline cryomilled powders. Pure bending fatigue tests have been performed and the samples have been

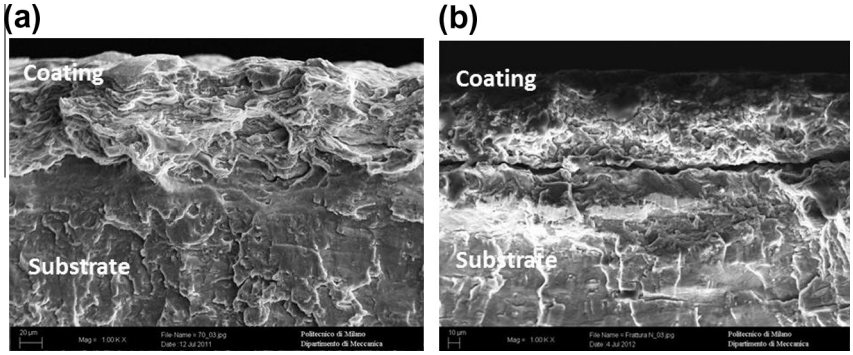

Fig. 8. SEM images of the fracture surface showing the interface for the samples coated by (a) Al7075 and (b) cryomilled Al7075.

examined through microstructural analysis, X-ray diffraction crystallite size and residual stress measurements, microhardness and surface roughness measurements. According to the obtained results, the following conclusions can be drawn:

- X-ray diffraction measurements show the presence of compressive residual stresses in both deposited material and the substrate.
- Microhardness measurements of coated samples, as expected, indicate considerable difference between the deposited material and the substrate hardness.
- Scanning electron microscopy observation of the samples' cross section indicates a porous coating structure in case of sample coated with cryomilled powder, while the sample coated with microcrystalline powder shows almost no porosity; this difference can be due to the coating parameters that have been equally set for both powders. It is anticipated with optimization of coating parameters for cryomilled powder, a similar non porous coating can be obtained.
- Fatigue test results show fatigue strength improvement for the coated series with respect to grit blasted samples; this fatigue strength improvement can be attributed to the contribution of the coating and work hardening effect induced by grit blasting and particle impacts. It can imply that the delaminations observed in case of samples coated with cryomilled powders have occurred at higher stresses. Considering that compressive residual stresses had lower values in coated samples compared to the just grit blasted one, the fatigue strength improvement cannot be just due to the presence of compressive residual stresses.
- Gradual increase in surface roughness parameters from grit blasted specimens to the ones coated by the microcrystalline powder and eventually the series coated by nanocrystalline powder can have deteriorating effect on fatigue strength of the specimens.
- Samples coated by cryomilled Al7075 nanocrystalline powder show very limited fatigue strength improvement with respect to samples coated by microcrystalline Al7075 powder; this limited improvement can be mainly due to the high porosity of the nanocrystalline coating compared to the one obtained by microcrystalline powder.

Based on these points, both spraying parameters and material properties seem to have considerable effect in the final fatigue strength. Fatigue strength enhancement for nanocrystalline coatings could be expected by changing the process parameters in order to reduce/eliminate the coating porosity and the surface roughness.

References

[1] Hanlon T, Kwon YN, Suresh S. Grain size effects on the fatigue response of nanocrystalline metals. Scripta Mater 2003;49:675–80.
[2] Ibrahim A, Lima RS, Berndt CC, Marple BR. Fatigue and mechanical properties of nanostructured and conventional titania (TiO2) thermal spray coatings. Surf Coat Technol 2007;201:7589–96.
[3] Champagne V. The cold spray materials deposition process, fundamentals and application. Woodhead Publishing; 2007.
[4] Ghelichi R, Bagherifard S, Guagliano M, Verani M. Numerical simulation of cold spray coating. Surf Coat Technol 2011;205:5294–301.
[5] Ajdelsztajn L, Jodoin B, Schoenung JM. Synthesis and mechanical properties of nanocrystalline Ni coatings produced by cold gas dynamic spraying. Surf Coat Technol 2006;201:1166–72.
[6] Phani GSPS, Vishnukanthan V. Effect of heat treatment on properties of cold sprayed nanocrystalline copper alumina coatings. Acta Mater 2007;55:4741–51.
[7] Guagliano M, Ghelichi R, Bagherifard S, Fernàndez Parienete I, Vezzù S. Effect of shot peening on residual stresses and surface work-hardening in cold sprayed coatings. Key Eng Mater 2010;417–418:397–400.
[8] Ghelichi R, MacDonald D, Bagherifard S, Jahed H, Guagliano M, Jodoin B. Microstructure and fatigue behavior of cold spray coated Al5052. Acta Mater 2012;60:6555–61.
[9] Padilla HA, Boyce BL. A review of fatigue behavior in nanocrystalline metals. Exp Mech 2010;50:5–23.
[10] Price TS, Shipway PH, McCartney DG. Effect of cold spray deposition of a titanium coating on fatigue behavior of a titanium alloy. J Thermal Spray Technol 2006;15:507–12.
[11] Sansoucy E, Kim GE, Moran AL, Jodoin B. Mechanical characteristics of Al–Co–Ce coatings produced by the cold spray process. J Thermal Spray Technol 2007;16:651–60.
[12] AL-Mangour B, Dallala R, Zhim F, Mongrain R, Yue S. Fatigue behavior of annealed cold-sprayed 316L stainless steel coating for biomedical applications. Mater Letter 2013;91:352–5.
[13] Mahmoudi H, Jahed H, Villafuerte J. The effect of cold spray coating on fatigue life of AZ31B. In: 9th International conference on magnesium alloys and their applications, Vancouver, BC, Canada, 2012.
[14] Legoux L, Irissou E, Moreau C. Effect of substrate temperature on the formation mechanism of cold sprayed aluminum, zinc, and tin coating. J Thermal Spray Technol 2007;16:619–27.
[15] Ning XJ, Jang JH, Kim HJ, Li CJ, Lee C. Cold spraying of AlSn binary alloy: coating characteristics and particle bonding features. Surf Coat Technol 2008;202:1681–7.
[16] A. specification metals material data sheet; 2011. <http://asm.matweb.com>.
[17] Maev R Gr, Leshchynsky V. Introduction to low pressure gas dynamic spray. WILEY-VCH Verlag GmbH & Co. KGaA; 2008.
[18] ASTM B593–96 (Reapproved 2009), Standard test method for bending fatigue testing for copper–alloy spring materials; 2009.
[19] Ghielmetti C, Ghelichi R, Guagliano M, Ripamonti F, Vezzù S. The design of a fatigue test machine for high frequency applications. Procedia Eng 2011;10:2892.
[20] Dixon W, Massey F. Introduction to statistical analysis. McGraw-Hilll; 1969.
[21] Brownlee KA, Hodges JL, Rosenblatt M. The up-and-down method with small samples. J Am Stat Assoc 1953;48:262–77.
[22] ASTM standard E739-10. Standard practice for statistical analysis of linear or linearized stress life (S–N) and strain life (e–N) fatigue data; 2010. doi: <http://dx.doi.org/10.1520/E0739-10>.
[23] DeKeijser Th H, Langford JI, Mittemeijer EJ, Vogels ABP. Use of the Voigt Function in a single-line method for the analysis of X-ray diffraction line broadening. J Appl Cryst 1982;15:308–14.
[24] Mittemeijer EJ, Welzel U. The state of the art of the diffraction analysis of crystallite size and lattice strain. Z. Kristallogr 2008;223:552–60.
[25] ISO 4278: Geometrical Product Specifications (GPS) – surface texture: profile method terms, definitions and surface texture parameters, 1st ed.; 1997.